



Investigating Wind Direction Influence on Wind-Generated Waves Using Delft 3D for Gaza Strip Coast

Anass Alqatanani¹, Ayşe Yeter Günal¹, M.Sobhi Alasta¹, Abdallah Jaroun¹, Adnan Al-Masri²

¹Department of Civil Engineering, University of Gaziantep, Gaziantep, Turkey.

²Department of Civil and Environmental Engineering, German Jordanian University, Amman, Jordan.

ARTICLE INFO

Article history:

Received 27/08/ 2022.

Received in revised form 20 /10/2022.

Accepted 24 /10/ 2022.

Available online 29/ 12 / 2022

Keywords:

wind-generated waves

Delft 3D

Gaza Strip Coast

ABSTRACT

Wind and water levels influence wave overtopping and consequent coastal flood threat, which is especially important in hyper-tidal bays where even modest variations in wave heights may be devastating if they coincide with high tides. The influence of wind and wave characteristics on wave propagation, as well as the sensitivity of significant wave height, are numerically investigated along the Gaza Strip's beachfront as an example. Wind waves with a high amplitude and short duration are susceptible to opposing winds, and their steepening effect varies throughout the bay shoreline, underlining the impact of shoreline geometry and bathymetry on wave hazard. The findings contribute to our existing knowledge of the complex interplay between wind and waves, as well as the crucial variables that maximize danger and hazard variability along the coastline. The findings of this study can assist port and harbor managers prevent financial losses due to downtime, influence sustainable coastal sea defense design, and better understand how wave danger may change in the future owing to shifting storm tracks. The findings can also be used to improve coastal infrastructure design and disaster response planning.

Two scenarios were investigated with a wind direction of 330 and 30. It seems that when the wind direction is 330, it produces a higher H_s of 1.2 m and relatively larger wave return period with a range of 12-22 s and a higher wave energy dissipation of 220 N/Ms. In contrast, when the wind direction is 30, it produces a smaller H_s of 1m with a short wave return period of 15-17s and smaller wave energy dissipation of 120 N/Ms. Overall, a wind direction of 30 has fewer occurring chances over the year but it seems to produce a destructive wave that are spread over the whole coast with a rapid return period.

DOI: [10.37650/ijce.2022.160204](https://doi.org/10.37650/ijce.2022.160204)

1. Introduction

In densely inhabited shorelines, the combination of high waves and fast winds with a long fetch may be disastrous (Desplanque & Mossman, 1999; Wolf, 2009). Strong water levels combined with high waves can generate an immediate uprush of water near the shore, pushing massive quantities of water over shorelines in a short amount of time (Eurotop et al., 2016; Hoeke et al., 2015).

This has consequences for wave inundation, and consequent coastal flooding, all of which are important for infrastructures, stakeholders, and property along the shore (Allsop et al., 2008; Bastidas et al., 2016; Thompson et al., 2017; Wolf, 2008).

A wind wave, also known as a wind-generated wave, is a water surface wave that emerges on the free surface of waterbodies in fluid dynamics. Wind waves are created when the wind blows over a fluid surface, with the fetch being the contact distance in the direction of the wind. Ocean waves can propagate thousands of kilometers

* Corresponding author. Tel.: +0-000-000-0000 ; fax: +0-000-000-0000.

E-mail address: anassalqatanani@gmail.com

before they reach the shore. Wind waves come in various sizes from tiny swirls to waves exceeding 30 meters (100 feet) high, with wind speed, duration, fetch, and ocean depth limiting their size.

The combined action of periodic high tides, waves, and wind cause local variations in water level in coastal areas across the world (Allsop et al., 2008; Bastidas et al., 2016; Letchford & Zachry, 2009). Heavy winds passing over the surface of shallow water produce waves that propagate toward the shore at different speeds and amplitudes depending on the water's depth (Wolf, 2009). Furthermore, sea level and wind waves affected coastal flooding in presence of ice cover (Johansson, 2022).

Coastal wave hazards can be dangerous to people and property when they coincide with higher wind speeds (Wolf, 2009) or at high tide. This is especially important in hyper-tidal bays, where the tidal range surpasses 6 m and even little variations in overall water levels and wave setup can be disastrous if they happen during high tide (Davis, 1964; Robins et al., 2016) also some researchers study the energy potency in many case studies (Warpindyasmoro, 2018; Atan et al., 2016). Moreover, wind waves hazards could reach reservoirs as the researcher (Zhang et al., 2022) reported.

The shoreline direction, geometry, and bathymetry funnel and magnify tidal wave propagation, resulting in large tidal ranges (Pye & Blott, 2014). Due to the enormous tidal range, extreme water depths allow waves to travel far up shore, causing waves to be felt over long areas of shoreline (Brown & Davies, 2010).

In densely inhabited and industrialized coastlines, accurate forecasting of nearshore waves is critical for reducing coastal wave and flood hazards. Correct predictions of coastal waves, as well as a knowledge of their potential effect, are crucial for providing accurate settings at the coastal boundary of flood hazard scenarios (of overtopping or inundation) used to guide management operations (Prime et al., 2016) or inside operational flood prediction systems (Hawkes et al., 2009).

This form of forecasting necessitates a thorough grasp of wave creation and development during high tide, as well as the effects of wind, wave type, and fetch. Wave hazard analysis and forecast can help us better understand the mechanisms that lead to maximum significant wave heights and the economic implications of waves near the shore. Wave overtopping during tidal high water, and consequent coastal flood danger, are frequently simulated using modeling methodologies to assess the possible effects for people, companies, and the natural and built environment.

Predicting maximum significant wave heights at high tide can help with coastal strategic planning and disaster response, enhance the layout of sea defenses and coastal infrastructure to decrease economic risks, and notify the public and decision-makers about extreme wave events to reduce loss of life. Many methods were used for forecasting and estimating in many fields, some researchers used artificial intelligence to forecast the ground water level (Ali et al., 2022) and maximum scour depth (Shaker and Gunal, 2021), while others used econometric models to forecast the demand (Hamed et al., 2022), also three-dimensional modeling were used in forecasting the maximum scour depth (Alasta et al., 2022). Moreover, many researchers used statistical and numerical methods to study the behavior of materials (Dheyab et al., 2017; Dheyaaldin et al., 2017).

2. Software

Delft3D is a modeling package that simulates flows, waves, and morphological changes in coastal, riverbank, and estuary systems (Lesser et al., 2004). A third-generation spectral wave model, Delft3D-WAVE, mimics the progression of wind-generated waves through time and space (Hydraulics, 2014). Delft3D-WAVE is based on the SWAN model Simulating Waves Nearshore (Ris et al., 1999; Daniels, et al., 2022), which is used to simulate short-crested waves in shallow coastal areas. The Navier-Stokes equations are used to derive this set of equations. Whereas these equations properly represent the flow of water, they are extremely complicated to solve without being simplified. When these equations are reduced to a form that can be solved with current computer capabilities, a new set of equations is discovered; these are the shallow water equations (refer equations 1-1, 1-2 and 1-3). The shallow water equations are made up of a system of equations that includes the governing equations and the equations of motion.

$$\frac{\partial u}{\partial t} + u \frac{\partial u}{\partial x} + v \frac{\partial u}{\partial y} + w \frac{\partial u}{\partial z} = -g \frac{\partial \zeta}{\partial x} + fv + 2 \frac{\partial}{\partial x} \left(v_t^H \frac{\partial u}{\partial x} \right) + \frac{\partial}{\partial y} \left(v_t^H \left(\frac{\partial u}{\partial y} + \frac{\partial v}{\partial x} \right) \right) + \frac{\partial}{\partial z} \left(v_t^V \frac{\partial u}{\partial z} \right) \quad (1.1)$$

$$\frac{\partial u}{\partial x} + \frac{\partial v}{\partial y} + \frac{\partial w}{\partial z} = 0 \quad (1.2)$$

$$\frac{\partial v}{\partial t} + u \frac{\partial v}{\partial x} + v \frac{\partial v}{\partial y} + w \frac{\partial v}{\partial z} = -g \frac{\partial \zeta}{\partial y} - fu + \frac{\partial}{\partial x} \left(v_t^H \left(\frac{\partial u}{\partial y} + \frac{\partial v}{\partial x} \right) \right) + 2 \frac{\partial}{\partial y} \left(v_t^H \frac{\partial v}{\partial y} \right) + \frac{\partial}{\partial z} \left(v_t^V \frac{\partial v}{\partial z} \right) \quad (1.3)$$

Where:

u : is the velocity in the x direction, or zonal velocity.

v : is the velocity in the y direction, or meridional velocity.

w : is the velocity in the z direction.

t : time.

H : is the mean height of the horizontal pressure surface.

g : is the acceleration due to gravity.

f : is the Coriolis coefficient associated with the Coriolis force.

k : is the viscous drag coefficient.

ν : is the kinematic viscosity.

The Delft3D-FLOW module solves the unsteady shallow water equations in either two (depth averaged) or three

2.1. Delft 3D-wave model calibration

The numerical wave model Delft3D-WAVE (SWAN) forecasts wave conditions from the model's offshore border to the near-shore regions. The flow/sediment transport model and the wave model interact and communicate in the near-shore regions. In order to replicate the coastal processes that are the focus of this work, an accurate depiction of the wave regime in the study region is necessary.

The Simulating Waves Nearshore Model (SWAN), created at Delft University of Technology in the Netherlands, has been successfully validated and verified in a variety of challenging laboratory and field experiments. It can be used to simulate the evolution of random, short-crested wind-generated waves in coastal waters, estuaries, tidal inlets, and lakes (Deltare, 2016b). Even when non-linear events predominate, the waves are described using the two-dimensional wave action density spectrum (e.g., in the surf zone). The model is able to convert offshore wave data into nearshore wave data while accounting for processes including wave refraction and diffraction caused by the presence of shoals, channels, or barriers; wave production by wind; wave dissipation by depth-induced breaking, white-capping, and bottom friction non-linear wave-wave interaction; and wave propagation through obstacles.

Delft3D-WAVE simulates a variety of physical phenomena, including bottom friction (using the JONSWAP formulation), refraction, depth-induced wave breaking, and wave dissipation owing to white capping (Delft Hydraulics, 2014). Many coastal and estuarine locations have effectively used the modelling system (Elias et al., 2012; Bastidas et al., 2016; Baresi et al., 2023).

2.2. Delft 3D wave module

The Delft3D-WAVE module may be utilized to model the emergence of wind-generated waves in coastal waters (which may include rivers, tidal entrances, barricade islands with tidal flats and channels). Delft3D's wave module evaluates wave propagation, wind-generated waves, non-linear wave-wave interactions, and dissipation for a specific bed topography, wind aspects, water elevation, and flow field in deep, moderate, and finite depth environments. The wave module in Delft3D is built on the SWAN numerical model of the third generation (Simulating Waves Nearshore). The purpose of the SWAN model is to simulate waves which are generated by the wind in coastal areas. The two-dimensional wave action density spectrum $N(\sigma, \Theta)$ is used to characterize waves in SWAN instead of the energy density spectrum $E(\sigma, \Theta)$. Because action density is conserved in the presence of flows but not energy density.

$$N(\sigma, \theta) = \frac{E(\sigma, \theta)}{\sigma} \quad (1.4)$$

N : Action density, E : Energy density, σ : Relative radian frequency, Θ : direction.

Delft3D-WAVE simulates wind-generated waves, dissipation caused by white capping, depth-induced wave breaking, bottom friction (using the JONSWAP formulation), and refraction (Hydraulics, 2014). Many coastal locations have effectively used the modelling system (Elias et al., 2012).

Delft3D-WAVE is used to simulate nearshore waves at the Gaza Strip coastline using a 2DH curvilinear model grid. The Delft3D-WAVE model's boundary was set far enough away from the shore to guarantee that boundary condition errors did not have a direct impact on the region of interest. The model grid resolution has been refined throughout the coast to increase the accuracy of significant wave height forecasting at the coastline, which is the study's primary focus. Grid-cell averaging and triangle interpolation were used to interpolate gridded bathymetry with a resolution of 50 m and a size of 10000 elements over the 2DH curvilinear grid. With a typical water level, substantial wave height, wave period, and wind speed parameters, the wave model is driven at one open border to the east.

A layered model grids is put up to fulfill this criterion and obtain a high degree of accuracy for the coast under

study (from the Gaza Strip coast line). The grid is forced using Palestinian central bureau of statistics Palestinian central bureau of statistics (PCBS) wave data. The grid is then utilized to transmit wave boundary conditions towards the coast, allowing wave data to be obtained close to the beach. Using the Delft Dashboard system, all of the data utilized as model input was transformed to 'Cartesian Coordinates.' WGS 84 / UTM21S is the zone that corresponds to the study area.

The Delft3D-WAVE module may be utilized to model the emergence of wind-generated waves in coastal waters (which may include rivers, tidal entrances, barricade islands with tidal flats and channels). Delft3D's wave module evaluates wave propagation, wind-generated waves, non-linear wave-wave interactions, and dissipation for a specific bed topography, wind aspects, water elevation, and flow field in deep, moderate, and finite depth environments.

2.3. Delft 3D methodology flow chart

The methodology of this study was to investigate the hydrodynamics of the study area by using Delft 3D. Different scenarios were further set up and simulated to predict the hydrodynamics of the selected area. This aspect can be summarized in Figure A-1.

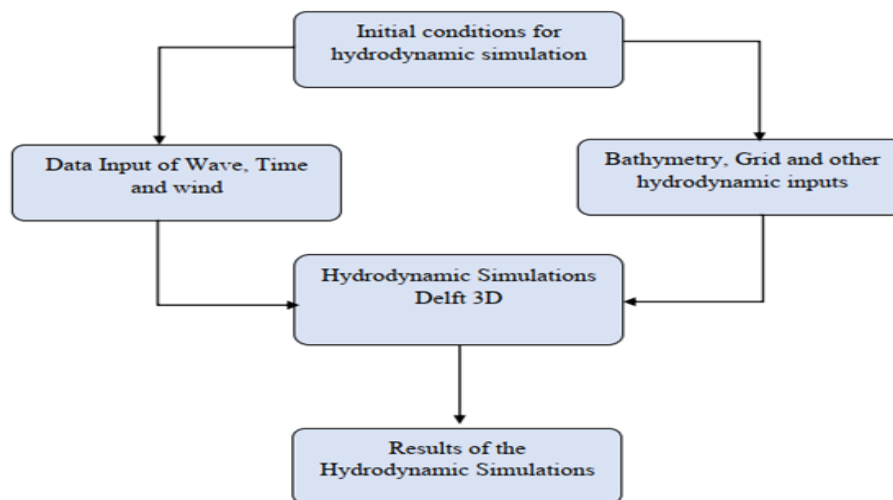


Figure A-1: Delft3D Methodology Flow Chart.

The SWAN model requires the following inputs: bathymetry, grid coordinates, bottom friction factor, wave breaking coefficients, diffraction coefficients, wind velocities, and height, period, direction, and directional spreading values for each wave event. The wave height, wave peak period, and wave direction are the SWAN model's outputs.

3. Materials And Methods

3.1. Study area

Gaza is a Palestinian enclave on the Mediterranean Sea's eastern shore. It has an 11-kilometer border with Egypt in the southwest and a 51-kilometer border with Palestine on the east and north. Figure 1, the Gaza Strip is 41 kilometers long, 6 to 12 kilometers broad, and 365 square kilometres in size. The Gaza Strip's highest point is approximately 105 meters above sea level. The Gaza Strip's population is estimated to be over 2 million people, with a growth rate of around 3.8 percent (Ramallah & Localities, 2016). The coastal and marine ecosystem of Gaza is under severe threat. Land scarcity resources, the area's geographical remoteness, and an inadequate environmental management system have all contributed to a slew of major issues.

3.2. Current status of the coastal zone

The Gaza coastline line is 42 kilometers long, 6 to 12 kilometers broad, and spans an area of 365 kilometers². It is located in the south-eastern section of Palestine and the Mediterranean Sea. Gaza is home to an estimated 1.3 million inhabitants.

The Gaza coastal zone is described as a belt of water and land that runs along the maritime coastline and is where activities collide. The coastal zone consists of the sand dunes in the south and north, the coastal cliffs (exposed Kurkar ridges) in the middle and north, the non-urban regions, the Wadis, and a portion of Gaza City. The land side of the coastal zone is around 74 km² in size, including 2.7 km² of beach.

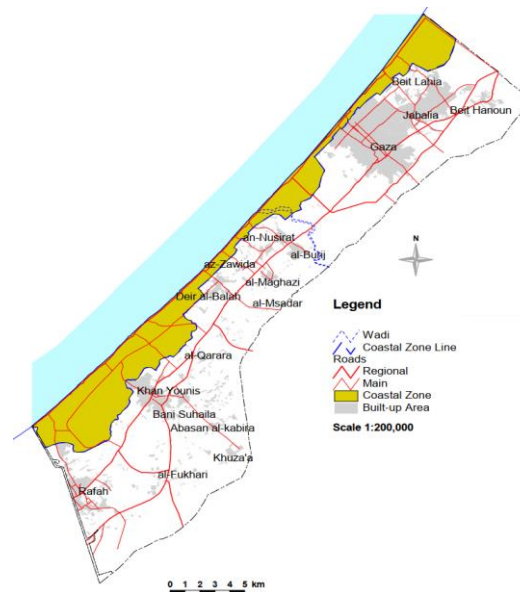


Figure 1. The Coastal Zone of Gaza.

3.3. Bathymetry of gaza cost

Figure 2 illustrates the bathymetry (geometry of the seafloor) off Gaza. The 100-meter depth line may be found 28 kilometers to the south and 14 kilometers to the north of Gaza. So, between the shore and the 100m depth line, the average seabed slope is around 1 in 200. The seabed dips rapidly to a depth of 1500 m beyond the 100 m depth line (outside Gaza waters).

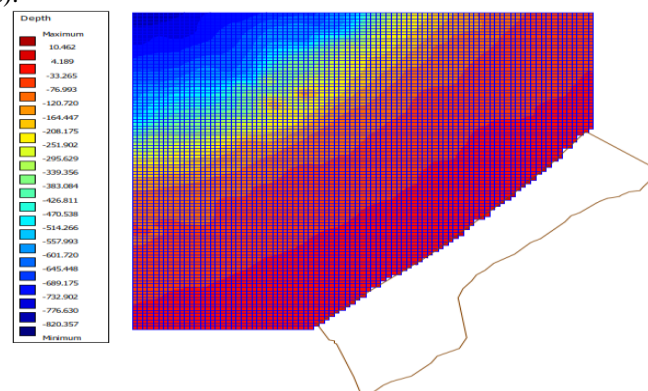


Figure 2 Gaza Strip Coastline Bathymetry combined with the mesh grid.

3.4. Waves and wind

Offshore wave and wind data utilized as input for Delft3D-WAVE comes from (Ramallah & Localities, 2016). Multiple scenarios are studied in this article, each with its own defined boundary data used to produce spatially variable wave conditions. The spatial varying boundary conditions were important for this study because the coast under study is so extensive, utilizing the same wave data for the whole coast would be insufficient and likely result in ambiguous conclusions. The aim of exploring multiple scenarios is to find the most critical one, analyze it, and thus share crucial information for decision-makers to minimize the threat of wave propagation.

Generally, the average hourly wind speed in Gaza varies slightly throughout the year. The data for 2021 shows that the minimum annual mean of wind speed was 7.3 miles per hour in May, while the maximum annual mean was 8.6 miles per hour in February.

4. Modelling

4.1. Delft 3D-WAVE modelling

As the successor of the shallow water wave hindcast model (HISWA), the SWAN model is a full spectrum 2-dimensional wave propagation and generation program developed by Delft University of Technology. Deltares has integrated the SWAN model into their Delft3D software package, named Delft3D-WAVE. 2012 (Deltares). Delft3D-WAVE is a discrete spectral action balance equation-based third generation shallow water wave model. The model is completely spectral and handles for the whole range of wave frequencies and orientations, allowing for the simultaneous propagation of short-crested random wave fields from significantly divergent directions. The propagation of waves is based on linear wave theory, which takes currents into account. With state-of-the-art third generation formulations, the processes of wind production, dissipation, and non-linear wave-wave dynamics are clearly modeled. All-important physical processes of wave propagation, generation, and dissipation are included in the model, such as: 1- Variations in depth and currents producing refraction. 2- Shoaling and Wave growth due to wind. 3- Wave dissipation due to white-capping, surf-breaking and bottom friction. 4- Wave-blocking due to an opposing current. 5- Non-linear wave-wave interaction in deep and shallow water. Delft3D-WAVE does not explicitly represent diffraction, however in many circumstances, the impacts of directed spreading and wave development owing to wind outweigh diffraction effects. (Ris et al., 1999) provides a more detailed explanation of the SWAN wave model.

4.2. Modelling strategy

Due to the lack of recorded near-shore wave data, the Delft3D-WAVE model was utilized to calculate near-shore wave data using the existing offshore wave climate data.

In order to simulate wave conditions in the area of interest from the Gaza Strip coast line a Delft3D-WAVE model is set up. Bathymetry data was obtained from the Ministry of Environmental Affairs, and from the General Bathymetric Chart of the Oceans data base (Kapoor, 1981). The data was then integrated to create the model bathymetry. The wave and wind conditions acquired from the Palestinian central bureau of statistics (PCBS) 2016 as stated in section 2 are utilized to set the Delft3D-WAVE model's boundary conditions.

The Delft3D-WAVE model's boundary was set far enough away from the shore to guarantee that boundary condition errors did not have a direct impact on the region of interest. A layered model grids is put up to fulfill this criterion and obtain a high degree of accuracy for the coast under study (from the Gaza Strip coast line). The grid is forced using Palestinian central bureau of statistics (PCBS) wave data. Different wave scenarios to run the model were created, which are detailed in the following sections. The grid is then utilized to transmit wave boundary conditions towards the coast, allowing wave data to be obtained close to the beach. Using the Delft Dashboard system, all of the data utilized as model input was transformed to 'Cartesian Coordinates.' WGS 84 / UTM21S is the zone that corresponds to the study area.

4.3. Delft-3D wave model input

4.3.1. model grid

A spatial grid is required by the Delft3D-WAVE model in order to compute wave propagation. As previously indicated, a system of large wave grids is used in this study to provide adequate precision in the area of interest. The grid area includes more than just the coastal area of Gaza Strip. The large wave grid is rectangular shaped and consists of a 100 of grid cells in M-direction and 100 Number of grid cells in N-direction with a total of 10000 grid elements, The bigger the grid the more precise it becomes and thus more sufficient accuracy. Figure 2. The local Wave Grid was used to examine wave propagation from the open ocean to the nearshore region.

4.3.2 Model Bathymetry

For the Delft3D-WAVE model to adequately simulate wave propagation and transformation towards the area of interest, good bathymetric data is required. Bathymetric data of the Gaza Strip shoreline was gathered from Palestinian Ministry of Environmental Affairs (ME nA). A more detailed bathymetry produces more accurate and

reliable findings. The data had to be digitalized in order to create a bathymetry file; each contour line of the map was saved as a 'x, y, z' file and then calibrated with the same point of reference to improve precision. The tool used to digitalize the data was Global Mapper, which was supplemented by a MATLAB script to generate the bathymetry file. After all of the depths had been calibrated, a file containing all of the data points was put into the Delft3D-QUICK IN suite, where it was edited and combined with the bathymetric data. Triangular interpolation and grid cell averaging were employed to interpolate the depth points. The bathymetry for the wave model grid is shown in Figure 2.

4.4. Model implementation

In order to execute the combination of the action equation given in SWAN in all five dimensions (time, geographical space (x,y), and spectral space (σ, θ)), Finite Difference Schemes were utilized. The time is excluded from the calculations since SWAN is used in fixed mode in Delft3D-WAVE. The geographical space is discretized using a rectangular grid with constant resolution in x and y.

Constant dimensional resolution and relative frequency resolution $\Delta\sigma/\sigma$ are used to discretize the spectrum. The discrete frequencies in SWAN are specified by a constant low frequency cutoff and a constant high frequency cutoff. A diagnostic (F^{-m}) tail is inserted above the high frequency cutoff for calculating wave interactions. Longer time steps are possible with implicit schemes, and the model is reliable.

SWAN supports grid nesting, and many grid resolutions can be incorporated in a single model run. Nesting is the concept of using a coarse grid for a wider region and a finer grid for a smaller field of concern. In the model input specification, the coarse and fine grids must be linked appropriately.

Independent bathymetry data for the primary and nested grids are required by the model. The model simulation results may be received in a variety of forms, including water depth (m), significant wave height (m), mean wave direction (deg.), peak wave period (s), directional spreading of waves (deg.), and the root mean square value of the highest orbital motion towards the bottom (m/s).

4.5. Boundary conditions

In the Delft3D-WAVE model, the spectral resolution in both orientation and frequency space must be determined for each computational grid. The frequency space is defined by a minimum and maximum frequency outside of the predicted lowest and peak frequency for the simulated area.

Apart from the frequency range, the number of frequencies to be considered in this range for computations must be specified as input. A total of 24 frequencies were determined in this study.

The whole 360-degree range can be defined in the directed space. Furthermore, the number of distinct directions must be provided. A resolution of 50 was used for this study.

In SWAN, boundary parameters may be presented in two aspects: 1. by the whole side orientation (north, northeast, southwest, etc.) and 2. by a section from a corner along a side (given by grid or x-y coordinates).

Boundary conditions are defined on both sides of the upper left corner of the computational grid, which is on the up-wave side of wave propagation, in this study.

The southwest border is defined by its orientation and has uniform wave boundary characteristics. The lateral border between land and deep sea on the northwest side is defined by segments and features space-varying wave boundary conditions.

The wind and wave propagation directions are found in a restricted sector in the north-west quadrant, ranging from 300° to 330° , according to the offshore data (Figure 3). A limited band of directional dispersion exists.

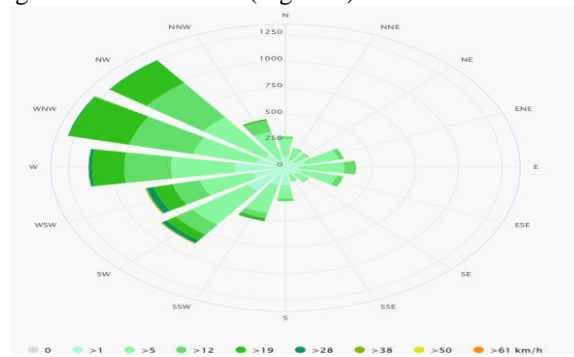


Figure 3 Annual Wind Rose offshore of Gaza Strip coastline.

The mean direction for the nesting and non-nesting seasons was estimated to be of comparable size. The influence of wind variability was investigated using wind conditions that corresponded to typical and severe situations.

In addition to the local boundary conditions, the simulated area was given time-varying winds and water levels to account for local wave production and water depth fluctuations owing to tides.

4.6. Delft3d -wave run

Delft3D-WAVE runs were performed using version 4.04.02 of Delft3D-WAVE, which was based on the 'MDW' files created, which contained wave and wind statistics, as mentioned in the preceding section. During the wave model application procedure, different coefficients and variables were altered; each run consisted of altering one variable to see the influence on wave propagation, such as bottom friction, depth induced breaking coefficients, and non-linear interaction coefficients. Different procedures were also turned on and off to see how they affected the outcome (Table 1).

Table 1 Delft3d-WAVE parameters.

Diffraction	Wind growth	White capping	Quadruplets	Refraction
De-activated	Activated	Activated	Activated	Activated
Wave set-up	Forces	Depth induced breaking	Non-linear triad interactions	Bottom friction
Activated	Radiation stress	Activated	Activated	Activated
		Alpha: 1	Alpha: 0.1	Type: JONSWAP
		Gamma: 0.73	Beta: 2.2	Coefficient: 0.067

5. Delft 3d Results and Discussion

5.1. Model results

The Delft3D WAVE (SWAN) model generates results for major wave parameters in the model domain at computational grid locations. For the current study, the findings of significant wave heights, mean wave direction, peak duration, dissipation rate, 1D spectrum, were analyzed.

The model simulations were performed for exceptional situations, two scenarios have been investigated with different wind direction of 330° at the first scenario and 30° at the second scenario and the findings are initially provided individually for these scenarios, followed by a comparison analysis based on context and relevance. The primary focus of this research is on shoreline wave conditions and wave energy dissipation along the coastline. The form and orientation of the Gaza coastline to the oncoming waves from the north west, as well as the shoreline depth contours, will impact wave refraction and diffraction, as well as energy transfer on the coastline edges.

For the first Scenario, Figure 4 illustrate the most common wave class that may be formed with a boundary Hs of 5.2m. This situation was forced by employing an offshore environment with northwest wave heights.

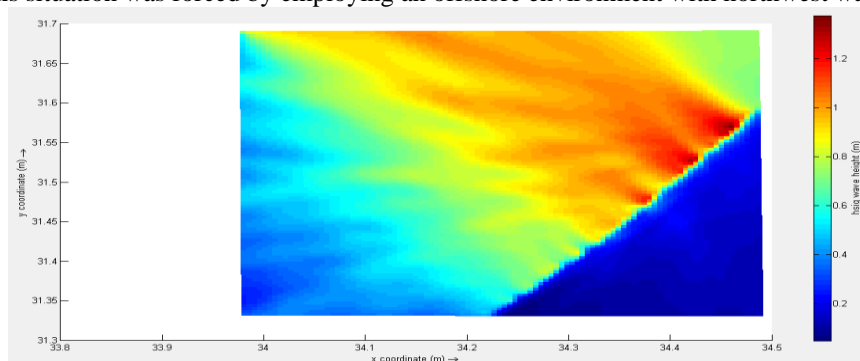


Figure 4 Significant Wave Height occurring once in 2 years at a direction of 330°.

The wave heights offshore in the northeast corner are the highest, reaching $H_s=1.2\text{m}$, while the area in the southwest has an offshore border with wave heights of roughly 0.6m , as shown in the image. Wave heights near the shore, particularly in the south region, begin to lose energy as they approach the coast, and as a result, wave heights near the coast are shorter (0.6m). In contrast, the north section waves kept their energy along the beach with a significant height of 1.2m . This is because the boundary orientation in this case is northwest and the wave direction is set to 330 degrees.

When the direction of the wave changed to 30° the highest value for the H_s was 1m along the shoreline but the distribution of the highest value of the significant wave was prominent near the coastline from south to north and for the most patches of the wave, the wave kept its energy in most parts of the wave expect in a small area in the northeast when the significant height reached a lowest value of 0.4m . Figure 5

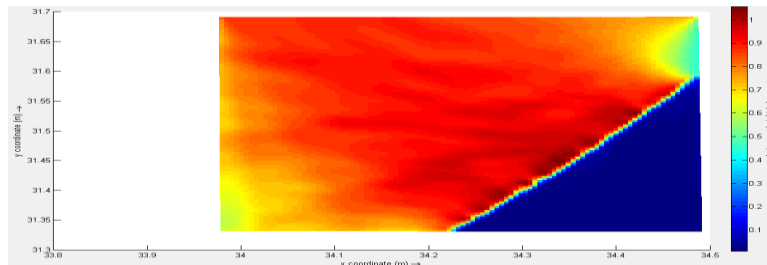


Figure 5 Significant Wave Height occurring once in 2 years at a direction of 30° .

While the direction is 30 , the wind and wave directions are virtually aligned; it can be seen that the upper portion has an arriving direction from the north; a rotation of wind and wave conditions can also be noted when travelling south; almost reaching a West incoming propagation direction. Figure 6 and 7 represents the values of the propagating wave and wind conditions.

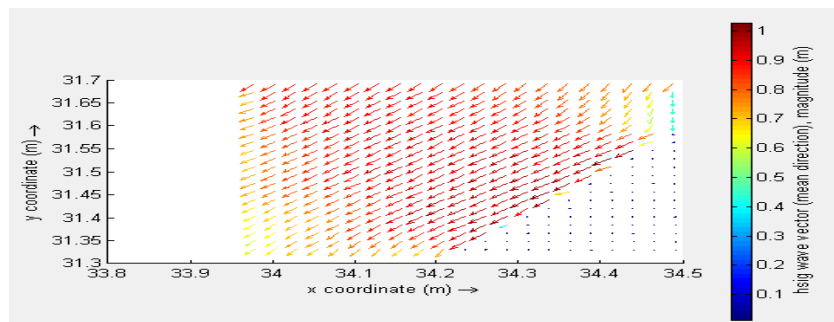


Figure 6 H_s wave vector direction and magnitude for a 30° propagation.

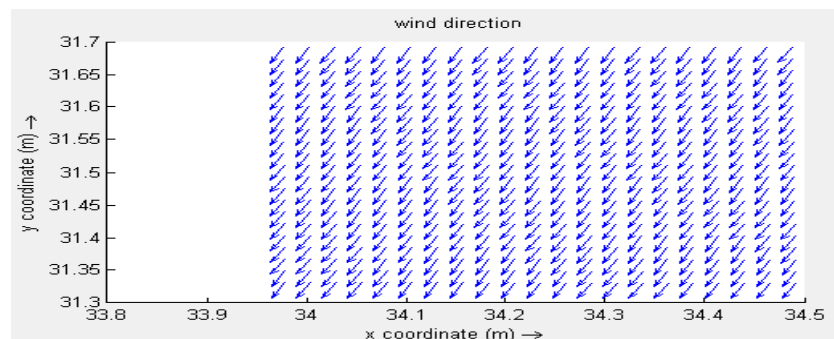


Figure 7 Wind direction of 30° propagation.

On the other hand, when the wave direction is at 330° , The wind and wave directions are not aligned in the same way they were in the prior direction. Waves are more prevalent in the northwest, whereas wind is more prevalent in the northeast. The wind directions are likewise shifted in the north border, where the prevailing direction is northwest, similar to the wave propagation direction. Figure 8 and 9.

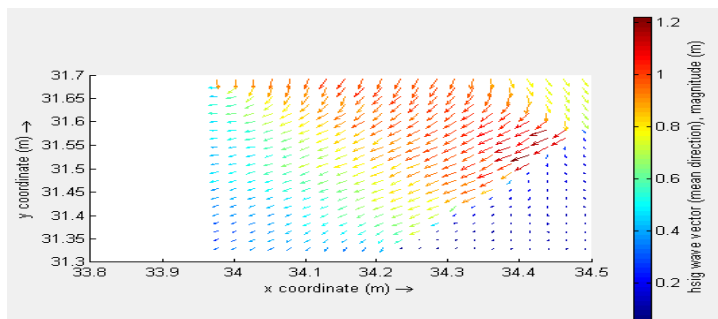


Figure 8 Hs wave vector direction and magnitude for a 330° propagation

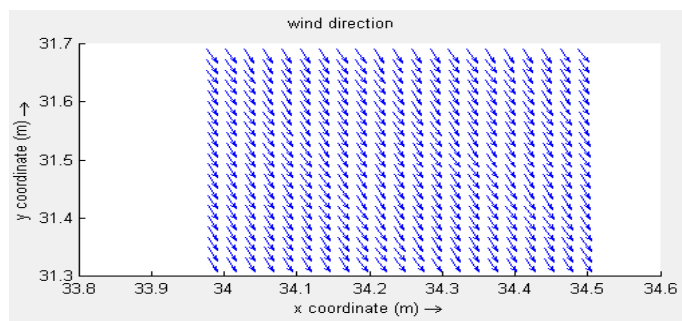


Figure 9 Wind direction 330° propagation.

The 330° waves have wave periods ranging from 12 to 22 seconds, and the distribution of bigger waves matches the distribution of larger periods. The north section, particularly the bay region, has shorter periods. Comparing the wave periods for the 30° waves they ranged from 15 to 17 seconds only which means waves are regenerating somewhat faster than the 330 waves. Figure 10 and 11.

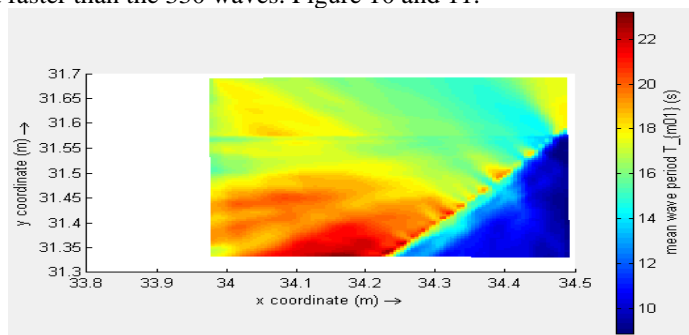


Figure 10 Mean wave period for a 330° propagation

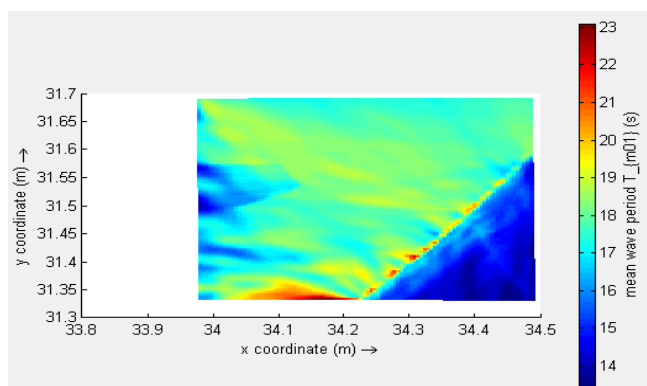


Figure 11 Mean wave period for a 30° propagation.

5.2 Conclusion

To sum up, two wave propagation directions angel of 30° and 330° for the most occurring scenario (1 in 2 years) , the magnitude of the significant wave height seems to be varying depending on the wave orientation angel with the same boundary conditions, when the wave direction vector align with the wind direction the value of the significant wave height appears to be less when the wind direction is on the opposite direction at a 330°, as for Gaza strip the wind rose direction during the year is at 300° to 330°, in other words the significant wave height will be constantly a little bit higher according to this wind direction.

The significant wave height H_s is just an indicator of the of the Maximum wave height H_{max} , which is approximately equal to two times H_s . While the majority of waves are less than the significant wave height, it is theoretically conceivable to meet a wave that is substantially larger, notably if people are out in the water for an extended period of time. It's expected that one out of every 3000 waves will exceed double the height of the significant wave height, or nearly three times per 24 hours.

In all maritime forecasts, the local authority should disseminate a note that maximum waves may be twice the relevant wave height as a reminder of this key safety principle.

This study employed the Delft3D WAVE standalone process averaged spectral wave model based on SWAN to convert waves from offshore to nearshore. At the lack of any measurable data on waves in the nearshore, the research uses default model settings to offer a quantitative and relative evaluation of the spread of significant wave heights and wave energy density, with an emphasis on wave energy dissipation over the shore.

Wind generation, non-linear trade interactions, white capping, refraction, Quadruplets, frequently shift, bottom friction, and depth induced wave breaking were all turned on in the Delft3D WAVE model. Due to grid size resolution concerns, the wave setup was turned off. The simulations used 36 di-rectional bins ranging from 0 to 360 degrees and 24 linearly distributed frequency bins ranging from 0.03 to 1.42 Hz. The formulation was used to describe depth constrained wave breaking, with the default value of $\gamma=0.73$. The near-shore wave climate was derived using the wave propagation model (Delft3D-WAVE), which was driven using offshore wave data (Battjes& Janssen, 1978). Based on the two scenario that were investigated it was concluded that:

- 1- In the 330-propagation direction, Wave energy dissipation is very significant in the north east section of the coast with a maximum magnitude of 220 N/ms but it's not well spread, due to the large area of very shallow waters. Figure 12

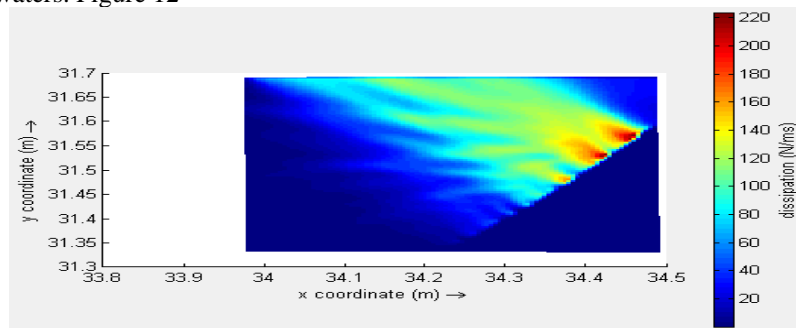


Figure 12 Wave Dissipation.

On the other hand, in the 30-propagation direction the wave energy dissipation drops to the half in value with a maximum value reached of 120 N/ms, but unlike the first direction it is well spread across the whole shore. Figure 13

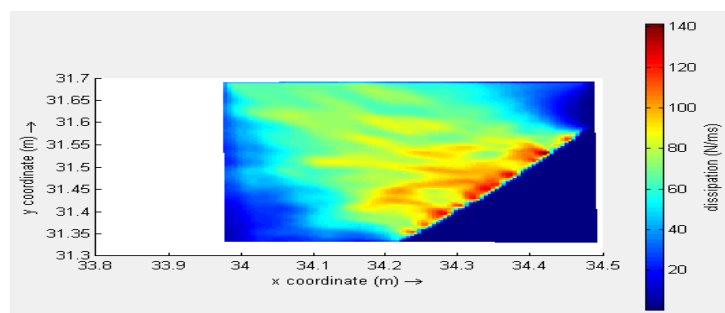


Figure 13 Wave Dissipation.

2-In the 330 directions, the wave heights offshore in the northeast corner are the highest, reaching $H_s=1.2\text{m}$, while the area in the southwest has an offshore border with wave heights of roughly 0.6m. Wave heights near the shore, particularly in the south region, begin to lose energy as they approach the coast, and as a result, wave heights near the coast are shorter (0.6m). In contrast, the north section waves kept their energy along the beach with a significant height of 1.2 m. This is because the boundary orientation in this case is northwest and the wave direction is set to 330 degrees.

When the direction of the wave changed to 30° the highest value for the H_s was 1m along the shoreline but the distribution of the highest value of the significant wave was prominent near the coastline from south to north and for the most patches of the wave, the wave kept its energy in most parts of the wave expect in a small area in the northeast when the significant height reached a lowest value of 0.4m.

3- The magnitude of the significant wave height seems to be varying depending on the wave orientation angel with the same boundary conditions, when the wave direction vector align with the wind direction the value of the significant wave height appears to be less when the wind direction is on the opposite direction at a 330° , as for Gaza strip the wind rose direction during the year is at 300° to 330° , in other words the significant wave height will be constantly a little bit higher according to this wind direction.

4- The 330° waves have wave periods ranging from 12 to 22 seconds, and the distribution of bigger waves matches the distribution of larger periods. The north section, particularly the bay region, has shorter periods. Comparing the wave periods for the 30° waves they ranged from 15 to 17 seconds only which is relatively smaller since the magnitude of the significant wave height is somewhat less than the 330° significant wave heights.

The significant wave height H_s is just an indicator of the of the Maximum wave height H_{max} , which is approximately equal to two times H_s . While the majority of waves are less than the significant wave height, it is theoretically conceivable to meet a wave that is substantially larger, notably if people are out in the water for an extended period of time. It's expected that one out of every 3000 waves will exceed double the height of the significant wave height, or nearly three times per 24 hours. In all maritime forecasts, the local authority should disseminate a note that maximum waves may be twice the relevant wave height as a reminder of this key safety principle.

6. Comparison With Recent Study

a recent study conducted by (Camarena Calderon, 2012) for wind generated waves modeling by delft 3d for the Buenos Aires coast, The model was implemented, forced by offshore wave/wind data from the NOAA Wave Watch data base, including 18 offshore wave/wind points used as spatially varying boundary conditions. The bathymetry of the area was built based on the nautical charts obtained from (Servicio de Hidrografia Naval, 2012), and the (GEBCO, 2008) global bathymetry. The NOAA wave and wind data was classified in 125 scenarios by using ORCA tools. The results of the model show a strong dominance of south storms was found, it was also concluded that the coast further north had a weaker wave climate and consequently smaller transport rates, mainly due to energy dissipation induced by bottom friction of the extensive shallow areas near the north section of the coast.

First, the most occurring wave class. This scenario was forced using an offshore climate with wave heights in the range of 1 to 1.5m and wave direction between 33.75° and 56.25° with respect to the north. the wave heights offshore in the southeast corner are the highest reaching an $H_s=1.4\text{m}$, while the section in the north has an offshore boundary with wave heights of around 1m. The corresponding periods for these conditions are very short, approximately 3 to 4 seconds. The wind and wave directions are almost aligned in this scenario.

The second most occurring scenario, is waves in the range of 1.5 to 2m, with incoming wave directions covering from 167.75° to 191.25° (Southeast waves). The significant wave height in this case is larger, especially for the southern section reaching the coast of Mar del Plata with a height in the range of 1.3 to 1.5 meters, while for the north section wave heights are significantly smaller (0.4 to 0.6m). The corresponding wave periods for these waves are in the range of 1.3s to 5.7s, the distribution of larger waves coincides with the distribution of larger periods. Shorter periods are found in the north section, especially in the bay area. For this scenario the wind and wave directions are not aligned as they were in the previously explained scenario.

The results of this study conducted by Camarena Calderon, R. A. (2012) align perfectly with the findings of this articles as it can be outlined that when the wind direction align with the wave direction the wave significant height is lower when the wind direction is from an opposite direction to the waves' direction with longer wave periods times. The fact that predicting wind generated waves is crucial for costal infrastructures development

taking into account physical, environmental and economic features. In addition, Coastal orientation had a significant effect on wave height variation in both studies, since less friction is encountered if the depth contours are perpendicular to the wave propagation direction.

7. Recommendation

The following are the main recommendations for future research, which are primarily related to data availability:

1. Using the bathymetry of the whole coast would enable the wave model to more accurately mimic the near-shore wave environment and improve the accuracy of the longshore and coastline outputs.
2. Wave buoys might be placed along the coast to collect data on near-shore waves. Additionally, it would offer a collection of comparison data to verify the predicted wave environment based on offshore data.
3. Perform monitoring campaigns to gather data on the retreat and advancement rates of the shoreline along the coast, including thorough near-shore bathymetries in the most pertinent sites around the Gaza Strip coast.
4. The numerical wave model Delft3D-WAVE (SWAN) is used to forecast wave conditions from the model's offshore border to the nearshore regions. The flow/sediment transport model and the wave model interact and communicate in the nearshore regions. In order to replicate the coastal processes that are the focus of this work, an accurate depiction of the wave regime along the study region is necessary.

References

- Allsop, W., Bruce, T., Pullen, T., & Van der Meer, J. (2008). Direct hazards from wave overtopping-the forgotten aspect of coastal flood risk assessment?
- Alasta, M. S., Ali, A. S. A., Ebrahimi, S., Ashiq, M. M., Dheyab, A. S., AlMasri, A., ... & Khorram, M. Modeling of Local Scour Depth Around Bridge Pier Using FLOW 3D.
- Ali, A. S. A., Ebrahimi, S., Ashiq, M. M., Alasta, M. S., & Azari, B. (2022). CNN-Bi LSTM neural network for simulating groundwater level. *Environ Eng*, 8, 1-7
- Bastidas, L. A., Knighton, J., & Kline, S. W. (2016). Parameter sensitivity and uncertainty analysis for a storm surge and wave model. *Natural Hazards and Earth System Sciences*, 16(10), 2195-2210.
- Battjes, J. A., & Janssen, J. (1978). Energy loss and set-up due to breaking of random waves. *Coastal Engineering Proceedings*(16), 32-32.
- Baresi, E. S., Wiyono, R. U. A., & Widiarti, W. Y. (2023). Wind-Generated Wave Simulation on Payangan Beach Utilizing DELFT3D. In *International Conference on Rehabilitation and Maintenance in Civil Engineering* (pp. 619-628). Springer, Singapore.
- Brown, J., & Davies, A. (2010). Flood/ebb tidal asymmetry in a shallow sandy estuary and the impact on net sand transport. *Geomorphology*, 114(3), 431-439.
- Daniels, T., Fearon, G., Vilaplana, A., Hewitson, B., & Rautenbach, C. (2022). On the importance of wind generated waves in embayments with complex orographic features—A South African case study. *Applied Ocean Research*, 128, 103355.
- DAVIES, J. (1964). A morphogenetic approach to world shorelines, *Zeit. f. In: Geomorph.*
- Desplanque, C., & Mossman, D. J. (1999). Storm tides of the Fundy. *Geographical Review*, 89(1), 23-33.
- DHEYAALDIN, M. H., ÖZAKÇA, M., & DHEYAB, A. S. (2017). Effect of stiffeners on structural behavior of steel liquids tank. *The International Journal of Energy and Engineering Sciences*, 2(3).
- DHEYAB, A. S., DHEYAALDIN, M. H., & ÖZAKÇA, M. Numerical Investigation of Structural Behavior Of Fiber Reinforced Polymers Filled Sandwich Panels
- Elias, E. P., Gelfenbaum, G., & Van der Westhuysen, A. J. (2012). Validation of a coupled wave - flow model in a high - energy setting: The mouth of the Columbia River. *Journal of Geophysical Research: Oceans*, 117(C9).
- Eurotop, J., van der Meer, W., Allsop, T., De Rouck, J., Kortenhaus, T. A., Pullen, H., Troch, P., & Zanuttigh, B. (2016). *Eurotop: Manual on Wave Overtopping of Sea Defences and Related Structures—an Overtopping Manual Largely Based on European Research, but for Worldwide Application*. In: Available at: www.overtopping-manual.com.

- Johansson, M. M., Björkqvist, J. V., Särkkä, J., Leijala, U., & Kahma, K. K. (2022). Correlation of wind waves and sea level variations on the coast of the seasonally ice-covered Gulf of Finland. *Natural Hazards and Earth System Sciences*, 22(3), 813-829.
- Hamed, M. M., Al-Masri, A., Dalala, Z. M., & AlSaleh, R. J. (2022). Modeling the Time Duration Until the Adoption of Residential Rooftop Solar Photovoltaic Systems. *Journal of Energy Resources Technology*, 144(4).
- Hawkes, P., Tozer, N., Pullen, T., Scott, A., Flowerdew, J., Mylne, K., Xavier-Bocquet, F., & Horsburgh, K. (2009). Probabilistic coastal flood forecasting.
- Hoeke, R. K., McInnes, K. L., & O'Grady, J. G. (2015). Wind and wave setup contributions to extreme sea levels at a tropical high island: A stochastic cyclone simulation study for Apia, Samoa. *Journal of Marine Science and Engineering*, 3(3), 1117-1135.
- Hydraulics, D. (2014). *Delft3D-FLOW User Manual: Simulation of multi-dimensional hydrodynamic flows and transport phenomena. Including Sediments*, 1-683.
- Kapoor, D. (1981). General bathymetric chart of the oceans (GEBCO). *Marine Geodesy*, 5(1), 73-80.
- Lesser, G. R., Roelvink, J. v., van Kester, J. T. M., & Stelling, G. (2004). Development and validation of a three-dimensional morphological model. *Coastal engineering*, 51(8-9), 883-915.
- Letchford, C., & Zachry, B. (2009). On wind, waves, and surface drag. 5th European and African conference on wind engineering, Florence, Italy,
- Prime, T., Brown, J. M., & Plater, A. J. (2016). Flood inundation uncertainty: The case of a 0.5% annual probability flood event. *Environmental Science & Policy*, 59, 1-9.
- Pye, K., & Blott, S. J. (2014). The geomorphology of UK estuaries: The role of geological controls, antecedent conditions and human activities. *Estuarine, Coastal and Shelf Science*, 150, 196-214.
- Ramallah, P., & Localities, B. (2016). *Palestinian Central Bureau of Statistics*. In.
- Ris, R., Holthuijsen, L., & Booij, N. (1999). A third - generation wave model for coastal regions: 2. Verification. *Journal of Geophysical Research: Oceans*, 104(C4), 7667-7681.
- Robins, P. E., Skov, M. W., Lewis, M. J., Giménez, L., Davies, A. G., Malham, S. K., Neill, S. P., McDonald, J. E., Whitton, T. A., & Jackson, S. E. (2016). Impact of climate change on UK estuaries: A review of past trends and potential projections. *Estuarine, Coastal and Shelf Science*, 169, 119-135.
- Shakir Ali Ali, A., & Günal, M. (2021). Artificial Neur